

Sieving hydrogen based on its high compressibility

H. Y. Chen¹, X. G. Gong², Z. F. Liu³ and D. Y. Sun^{1*}

¹*Department of Physics, East China Normal University, Shanghai 200062, China*

²*Department of Physics, Fudan University, Shanghai-200062, China and*

³*Department of Chemistry and Center for Scientific Modeling and Computation,
Chinese University of Hong Kong Shatin, Hong Kong, China*

(Dated: October 21, 2018)

Abstract

A molecular sieve for hydrogen is presented based on a carbon nanotube intramolecular junction and a C_{60} . The small interspace formed between C_{60} and junction provides a size changeable channel for the permselectivity of hydrogen while blocking Ne and Ar . The sieving mechanism is due to the high compressibility of hydrogen.

With growing demand on clean energy, the production and separation of hydrogen with great amount represent a topic of intense interests. One of the straightforward and commercial ways to separate hydrogen is to use a specifically designed molecular sieve with high selectivity and permeability. Efforts on using the traditional molecular sieve, such as polymeric membrane, have been ongoing for some time and the progress has been made along this direction.[1, 2] However, the major problem related to polymeric membranes is the strong trade-off between selectivity and permeability.[1, 2] Thus, the search of new sieves or new methods to improve the permselectivity of hydrogen from mixtures is much needed to match the growing demand in the hydrogen energy.[3, 4]

In molecular sieves, the major mechanism for the filtration usually bases on the difference in size, shape or polarity of varies molecules in the mixture. H_2 has almost spherical shape and no polarity, thus the probable sieving mechanism for H_2 is limited to use its small size. Attempts to design sieves based on the size difference have been made over the past few years.[3, 4] This kind of sieve is quite useful for molecules with large size difference. However, for molecules having comparable sizes with H_2 , the efficient way for the separation is still lack of.

The purpose of this letter is to find an alternative mechanism to design sieves for hydrogen. We notice that hydrogen has a novel property, namely the highly compressible character, which is absent for most other molecules.[5, 6] A hydrogen molecule has only two electrons on fairly compact 1s orbitals, the van der Waals repulsion between two H_2 molecules is much weaker than typical, so that it is highly compressible all the way up to and above GPa pressure. The soft repulsion is also found for H_2 interacting with other systems, such as graphite.[29] The highly compressible character makes hydrogen have much more chances to diffuse at confinement space over other gases. Furthermore, H_2 is the lightest molecule in nature, at a given temperature, so H_2 could have higher mobility in confinement space than other gases. Considering the above two features, it is possible to design a molecular sieve to filtrate hydrogen.

The ideal candidate for current studies could be carbon nanotubes (CNTs) due to its tubular structures and small pore sizes. In fact, over the past few years, many studies have focused on the investigation of the selectivity and transport properties of light gases in CNTs.[7–11] However the use of CNTs as a molecular sieve for hydrogen is still a great challenge. If one hopes to directly use the pore of CNTs, the CNT should have comparable pore size with H_2 ($\sim 3\text{\AA}$). Such small pore size almost approaches to both theoretical predicated limitation and the smallest CNT fabricated in experiments.[12–14] Up to now, as far as we know, the reliable design based on CNTs is still

lack of.

To avoid the above mentioned limitation, we do not directly use the channel of CNTs, but the interspace formed between C_{60} and CNTs. The inset of Fig. 1(a) presents the geometry of the molecular sieve. It is made of an intramolecular junction and a C_{60} . To form the intramolecular junction between two tubes, the method presented in Ref.[15–19] is adopted. Combining the well-developed experimental techniques for producing junctions[20–22] and for inserting C_{60} into CNTs[23–25], our design could be easily fabricated. In current studies, the left tube is (20,0) CNT, which is larger than C_{60} , while the right one is (5,5) CNT, smaller than C_{60} . The interspace formed between C_{60} and CNTs could provide a nano channel for the separation of hydrogen using its high compressibility.

To compare the permselectivity of hydrogen with other gases, two typical gases are also considered, which are Ne and Ar . All the molecules/atoms have almost spherical shape and no polarity, the major difference is their size. Among these molecules, Ar is the one with largest diameter (about 3.8Å); while H_2 and Ne have the similar sizes of about 3.3Å and 3.1Å respectively. Because the difference in sizes is not prominent and H_2 even has larger size than Ne , the separation could be very difficult, even impossible in traditional molecular sieves. If hydrogen can be separated from those molecules mentioned above, this design could also work for most other types of molecules, such as CH_4 , N_2 and O_2 . It needs to be pointed out that, all the three molecules can easily pass both (20,0) and (5,5) CNTs.

To validate this molecular sieve, several calculations have been carried out. First, to check the size and stability of the narrow space formed between C_{60} and CNT, we have studied the absorption behavior of C_{60} . Second, to verify if a single H_2 molecule can easily pass the sieve without the highly compressibility emerged, the diffusion barrier for one molecule passing the sieve has been calculated. Third, to validate the importance of the high compressibility, a comparing study on the transport properties for each pure gas in the sieve is carried out. Finally, the permselectivity of H_2 mixed with other gases is also calculated. This work demonstrates that, if the highly compressible character of hydrogen are taken into account, our design does work as a molecular sieve for hydrogen.

We have addressed the above questions using molecular dynamic (MD) simulation. To calculate the permselectivity and flux, the molecular sieve with length about 36 Å is dipped into a reservoir, as shown in Fig.1(b). Two plates, labeled as A and B, are placed at the two boundaries of the reservoir perpendicular to the molecular sieve. These plates, made of the corresponding gas

molecules, are rigid with face-centered cubic (111) planes. In all simulations, plate B is fixed, while plate A is movable. In all studies, the system temperature keeps at 300 K by Nóse-Hoover thermostat.[26] The equations of motion are integrated by using the predictor-corrector algorithm with time step of 1 fs. Periodic boundary conditions are only applied in directions perpendicular to the CNTs. The pressure difference around C_{60} is defined as $\Delta P = P_{left} - P_{right}$, where P_{left} is fluidic pressure of the reservoir, and P_{right} keeps zero in all simulations. In current studies, ΔP is changed by placing the plate A at different positions. For each move of plate A, the large CNT is blocked by fixing a few atoms/molecules inside it for first 0.4 ns so that the fluid in the reservoir is fully equilibrated. Afterwards, all gas atoms/molecules are movable, and the system is simulated for about 0.6 ns to determine the flux of gases.

The interatomic potential between carbon atoms is the Tersoff-type many-body potential with parameters given by Brenner.[27, 28] The weak interaction between carbon atoms in CNTs and C_{60} is modeled by the Lennard-Jones (L-J) potential, $V_{vdW} = C_{12}/r^{12} - C_6/r^6$ with $C_6=20 \text{ eV}\text{\AA}^6$ and $C_{12} = 2.48 \times 10^4 \text{ eV}\text{\AA}^{12}$. Interactions between H_2 molecules are modeled by the Silvera-Goldman potential, which correctly reproduce the equation of states for H_2 in wide range of pressures.[5] The weak interaction between H_2 and carbon is described by the recently fitted potential by some of us,[29] which reproduces the results over a wide range of repulsive and attractive regions as calculated by high level *ab-initio* methods.[30] The interactions of *Ne* and *Ar* are L-J potential with the parameters taken from reference[31]. Within the pressure up to 1 GPa, the L-J potential could accurately predicate melting curve and other properties which are comparable to experimental results.[31, 32] The interactions of C-*Ne* and C-*Ar* are also L-J potential and calculated using Lorentz-Berthlot combination rules with parameters of C-C taken from Ref.[33].

Without filling any gases, there is one stable adsorption site for C_{60} around the intramolecular junction. Fig.1(a) shows the potential energy of the system as C_{60} moving along axial direction. At this stable adsorption site, C_{60} is right located at the axis center near the junction. The minimal distance between C_{60} and the junction is around 3.3 Å as indicated in the inset of Fig. 1 (a) labeled as 'interspace A'. The interlayer distance from C_{60} to tube wall is about 4.3 Å marked as 'interspace B'. The stable adsorption position is a reflection of the good geometric match between junction and C_{60} , namely, favorable interactions between pairs of C atoms on CNTs and C_{60} reach maximum. The adsorption energy is about 1.17eV lower than that for C_{60} far from the junction. The stable adsorption guarantees C_{60} staying near the junction, which is important for the current sieve. Due to the weak interaction between C_{60} and tube wall, C_{60} can be moved around the stable

position in a certain range, which forms a 'size changeable channel'.

The diffusion barriers for single molecule/atom passing the molecular sieve are calculated, which is plotted in Fig. 2(a). We find that, when the molecule locates at interspace A, the global potential maximum appears. As the molecule locates at interspace B (right above C_{60}), there is another local potential energy maximum (flat), which is more obvious for Ar . There is a strong correlation between the position of molecule/atom and displacement of the mass center of C_{60} . Fig. 2 (b) and (c) show the associated motion of the mass center of C_{60} as the molecule moving along the tube axial direction. As the molecule approaches to the interspace B, C_{60} is pushed backward and begins to move to the tube wall. The displacement of C_{60} produces increasing space for the molecule. It reaches the maximum as the gas molecule arrives interspace A. At the same time, the potential energy reaches the maximum. After the molecule passes interspace A, C_{60} is ready to move back to its equilibrium position. This implies that the energy barrier is mainly due to the displacement of C_{60} . The larger the displacement of C_{60} is, the higher the energy barrier is. For Ar , the displacement of C_{60} along radial/axial direction from the equilibrium position is around $1.61\text{\AA}/1.71\text{\AA}$, while for H_2 or Ne , the corresponding value is $1.35\text{\AA}/1.07\text{\AA}$ and $1.36\text{\AA}/1.08\text{\AA}$, respectively. The diffusion barrier for H_2 and Ne has the similar value around 0.44 eV (0.45eV for Ne and 0.43eV for H_2), which is lower than the barrier of 0.68eV for Ar . The diffusion barrier suggests that, for a single molecule/atom, it is very difficult to pass the molecular sieve at room temperature. As we will discuss below, if the high compressibility of hydrogen is emerged (plenty of H_2 molecules appear), the difference in transport behavior among H_2 , Ne and Ar will be significant.

In Fig. 3(a), we have shown the flux via ΔP for pure H_2 , Ne and Ar at 300 K separately. From this figure, one can see that, with the increase of pressure difference up to 1 GPa , only H_2 molecules are excluded out from the molecular sieve, while other gases (Ne and Ar) are blocked by C_{60} with zero permeation. As we have discussed that Ne has almost the same diffusion barrier as H_2 (see figure 2(a)). Thus, H_2 and Ne should have comparable chance to pass the sieve if the diffusion of the single atom/molecule dominates this process. However the permeability of Ne is much lower than that of H_2 . The mystery can be disclosed in terms of the high compressibility of hydrogen. It is well known that the diffusion rate is proportional to the inverse of the square root of molecular mass. However the mass issue is not enough to explain the transport difference between H_2 and Ne . On the contrary, the high compressibility of H_2 plays a key role. Comparing with Ne , this character is not quite obvious when few molecules appear or the pressure is low (figure 2 (a)).

With the increase of pressure, the high compressibility (both soft repulsion of $H_2 - H_2$ and $H_2 - C$) becomes more and more important.

The high compressibility makes H_2 have more chance to accumulate in interspace B. We have calculated the average number of molecules located within a narrow window around interspace B. This narrow window has the width of 4\AA along the axial direction and centered on C_{60} . Fig. 3 (b) shows the average number of molecules/atoms within this narrow window via ΔP . One can see that, the number of H_2 in this area is much more than Ne . And the number increases with the increase of ΔP . For Ne , even at 1 GPa, the number is less than two, which is several times smaller than that of H_2 . No Ar atom is found at interspace B even at 1 GPa. The molecules located at the interspace B will not only increase the chance moving to interspace A, but also lower the diffusion barrier due to the inward motion of C_{60} driven by the molecules located around interspace B. With growing number of H_2 moving into interspace B, H_2 is more easily to overcome the energy barrier and be excluded out.

To further verify that transport properties of hydrogen is dominated by the high compressibility, rather than the small mass of H_2 , we have carried out two additional calculations, which is shown in the inset of Fig. 3 (a). In the first run (long dashed line), the mass of H_2 is artificially enlarged ten times. In this case, we found that the flux is simply reduced according to the change of mass. In the second run (dot-dashed line), the interaction of H_2-H_2 and H_2-C is replaced by a typical L-J potential.[34] Our calculations show that, in this case, the transport of hydrogen is terminated.

The permselectivity of H_2 mixed with Ne and Ar is further studied separately. In this calculation, the number ratio is chosen as $H_2 : M$ ($M=Ne$ or Ar)= $1:1, 3:1, 9:1$. Fig. 4(a) and (b) shows the flux of two components mixed gases as a function of ΔP . One can see that, in all studied cases, the permeation of H_2 is nonzero and increase with the increase of ΔP . In all the simulations, there is no Ar atom found to pass the molecular sieve. In the mixture of H_2 and Ne , the flux of Ne , as the pressure difference raised up to around 0.6 GPa, becomes nonzero. However it is still much smaller than that for H_2 (Please see the Supporting Information for a animation of this process). Detailed studies show that, the leakage of a few Ne molecules is mainly 'abducted' by H_2 . That is, by chance, some Ne are surrounded by H_2 , these Ne atoms pass the molecular sieve associated with H_2 . For the mixture of three types of gas molecules (H_2, Ne and Ar) with the ratio of $1:1:1$, our calculations also show that, only H_2 pass through the molecular sieve when ΔP is in the range $0.2GPa \sim 0.6GPa$, as shown in Fig. 4 (c) (Please also see the Supporting Information for a animation of this process). Similarly a few of Ne also leak out from the molecular sieve as ΔP

raising up to 0.6 GPa. As ΔP up to 1 GPa, no *Ar* penetrates the molecular sieve during at least 1 ns simulation time.

The final question, which should be addressed, relates to the requirements on using the high compressible character of H_2 . For this purpose, we have checked the sieving function for hydrogen in a few combinations of intramolecular junction and C_{60} . Our results show that the position of C_{60} and the size of the interspace formed between the tube wall and C_{60} are the important factors. First, the size of interspace should not be too small, otherwise the leakage of H_2 is blocked. The size of interspace should also not be too large, otherwise other gases could penetrate and the high compressibility of H_2 plays less role. We found that the interspace between the tube wall and C_{60} should be around 3.5 Å, correspondingly, the radius of the larger CNT in the sieve around 16 Å is the ideal one. For the smaller tube, it needs to have enough space for hydrogen passing. Second, the potential well of C_{60} should not be too stiff, otherwise C_{60} could not move to produce more space. For example, the intramolecular junction formed between (20,0) and (10,0), which fills the requirements, also has the function as a molecular sieve. We believe that, besides of the current design, there could be many structures for using the high compressible character and the small mass of H_2 .

In conclusion, by taking the high compressibility of hydrogen into account, we have proposed a potential molecular sieve for hydrogen based on C_{60} and carbon nanotube intramolecular junction. Our calculations show that the narrow interspace formed between the tube wall and C_{60} provides a size changeable channel. The diffusion barriers for a single molecule/atom passing this channel are quite high (0.45 eV for Ne, 0.43 eV for H_2 , and 0.68 eV for Ar). The diffusion barriers imply that, for a single molecule/atom, it is difficult to pass the molecular sieve at room temperature. If plenty of H_2 appear (the high compressibility of H_2 is emerged), the transport behavior of H_2 , Ne and Ar is significant difference. Using molecular dynamics simulations, we have studied the permselectivity of H_2/Ar , H_2/Ne and $H_2/Ar/Ne$ mixtures. Our calculations show that no Ar is found to pass the sieve, while H_2 can pass the sieve with noticeable flux. A few Ne atoms can also leak out, however the amount is much smaller than H_2 . The selective permeation of H_2 is the result of the high compressibility of H_2 . The current design could be an alternative technique for the separating of H_2 from most of mixtures.

Acknowledgment. This research is supported by Key Project of Shanghai Education Committee, Shanghai Municipal Science and Technology Commission, the National Science Foundation of China. Z. F. L acknowledges financial support from the Research Grant Council of Hong Kong

through Project 402309. The computation is performed in the Supercomputer Center of Shanghai and the Supercomputer Center of ECNU.

Supporting Information Available. Two movies for the permselectivity process of hydrogen in a mixture. This material is available free of charge via the Internet at <http://pubs.acs.org>.

* Email address: dysun@phy.ecnu.edu.cn

- [1] Robeson, L. M. *J. Memb. Sci.* **1991**, 62, 165-185
- [2] Freeman, B. D. **1999**, 32, 375-380
- [3] Jiang, D.; Cooper, V. R.; Dai, S. *Nano Lett.* **2009**, 9, 4019-4024
- [4] Li, Y.; Zhou, Z.; Shen, P.; Chen, Z. *Chem. Commun.*, 2010, 46, 36723674
- [5] Silvera, I. F. *Rev. Mod. Phys.* **1980**, 52, 393 .
- [6] Hemley, R. J.; Mao, H. K. *Phys. Rev. Lett.* **1988**, 61, 857.
- [7] Skoulidas, A. I.; Ackerman, D. M.; Johnson, J. K.; Sholl, D. S. *Phys. Rev. Lett.* **2002**, 89, 185901
- [8] Challa, S. R.; Sholl, D. S.; Johnson, J. K. *J. Chem. Phys.* **2002**, 116, 814-824
- [9] Arora, G; Sandler, S. I. *Nano Lett.* **2007**, 7, 565-569
- [10] Liu, L.; Chen, X. *J. Phys. Chem. B* **2009**, 113, 6468-6472
- [11] Sharma, A.; Kumar, S.; Tripathi, B.; Singh, M.; Vijay, Y. K. *Int. J. Hydrogen Energy* **2009**, 34, 3977-3982
- [12] Zhao, X.; Liu, Y.; Inoue, S.; Suzuki, T.; Jones, R. O.; Ando, Y. *Phys. Rev. Lett.* **2004**, 92, 125502
- [13] Guan, L.; Suenaga, K.; Iijima, S. *Nano Lett.* **2008**, 8, 459-462
- [14] Peng, H. Y.; Wang, N.; Zheng, Y. F.; Lifshitz, Y. *Appl. Phys. Lett.* **2000**, 77, 2831-2833
- [15] Sun, D. Y.; Chen, H. Y.; Liu, J. W.; Gong, X. G.; Liu, Z. F. *Phys. Rev. B* **2009**, 79, 033403
- [16] Chen, H. Y.; Liu, Z. F.; Gong, X. G.; Sun, D. Y. *Microfluidics and Nanofluidics* DOI: 10.1007/s10404-010-0719-8.
- [17] Wu, G.; Li, B. W. *Phys. Rev. B* **2007**, 76, 085424
- [18] Rochefort, A.; Avouris, P. *Nano Lett.* **2002**, 2, 253-256
- [19] Legoas, S. B.; Coluci, V. R.; Braga, S. F.; Coura, P. Z.; Dantas, S. O.; Galvão, D. S. *Phys. Rev. Lett.* **2003**, 90, 055504
- [20] Rodríguez-Manzo, J. A.; Janowska, I.; Pham-Huu, C.; Tolvanen, A.; Krasheninnikov, A. V.; Nordlund, K.; Banhart, F. *Small*, **2009**, 5, 2710-2715

- [21] Li, Y.; Xie, S.; Zhou, W.; Bando, Y. *Carbon* **2003**, 41, 380-384
- [22] Jin, C. H.; Suenaga, K.; Iijima, S. *Nat. nanotechnology* **2008**, 3, 17-21
- [23] Smith, B. W.; Monthioux, M.; Luzzi, D. E. *Nature* **1998**, 396 323-324
- [24] Monthioux, M. **2002**, 40, 1809-1823
- [25] Jeong, G.-H.; Hirata, T.; Hatakeyama, R.; Tohji, K.; Motomiya, K. *Carbon*, **2002**, 40, 2247-2253
- [26] Frenkel, D. ; Smit, B. *Understanding Molecular Simulation: From Algorithms to Applications*, 2nd ed. (Academic press, San Diego, 2002).
- [27] Matsubara, K.; Sugihara, K.; Tsuzuku, T. *Phys. Rev. B* **1990**, 41, 969-974
- [28] Brenner, D. W. *Phys. Rev. B* **1990**, 42, 9458-9471
- [29] Sun, D. Y.; Liu, J. W.; Gong, X. G.; Liu, Z. F. *Phys. Rev. B* **2007**, 75, 075424
- [30] Ferre-Vilaplana, A. J. *Chem. Phys.* **2005**, 122, 104709
- [31] Choi, Y.; Ree, T.; Ree, F. H. *Phys. Rev. B* **1993**, 48, 2988-2991
- [32] Koči, L.; Ahuja, R.; Belonoshko, A. B. *Phys. Rev. B* **2007**, 75, 214108
- [33] Stan, G.; Bojan, M. J.; Curtarolo, S.; Gatica, S. M.; Cole, M. W. *Phys. Rev. B* **2000**, 62, 2173-2180
- [34] Insepov, Z.; Wolf, D.; Hassanein, A. *Nano Lett* **2006**, 6, 1893-1895

FIG. 1. (Color online) (a) The potential energy change of the molecular sieve as C_{60} approaching to the junction. The initial axial distance of C_{60} (the original of x-axis) is around 17\AA far away from the junction. The energy has been shifted so that the energy at initial position of C_{60} is zero. Inset: The top and horizontal views of the molecular sieve, which is composed with a carbon nanotube intramolecular junction and an encapsulated C_{60} . (b) The illustrations of the simulation system for calculating the flux/permeability of gases, where the plate B is fixed, while plate A is movable to tune the pressure difference around the sieve.

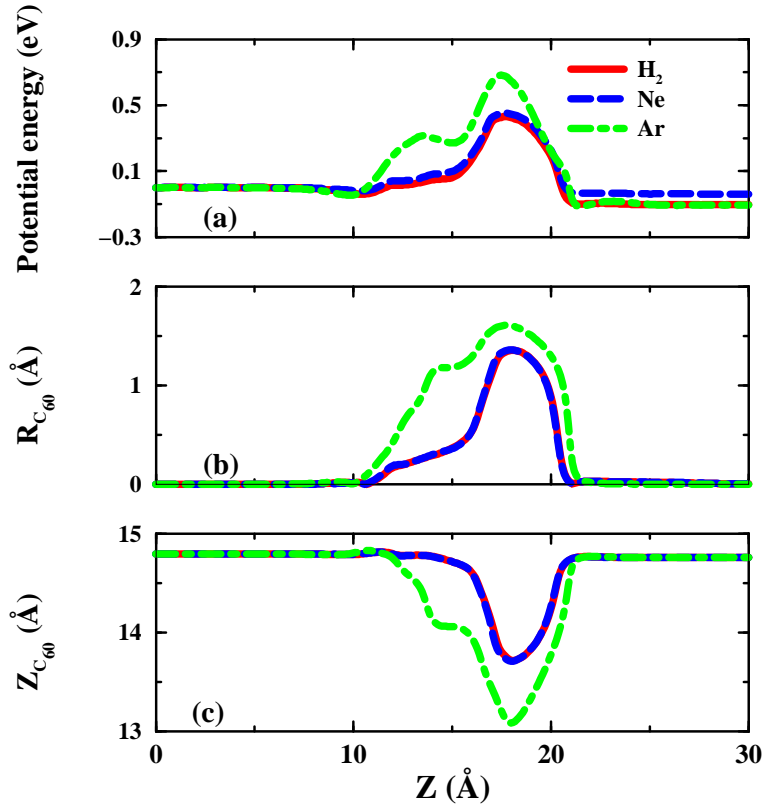


FIG. 2. (Color online) The potential energy change of system (a), the radial (b) and axial displacement (c) of C_{60} as the gas molecule moves along axial direction. The initial axial distance of molecule (the original of x-axis) is around 20\AA far away from the junction. The energy has been shifted so that the energy at initial position of molecule is zero.

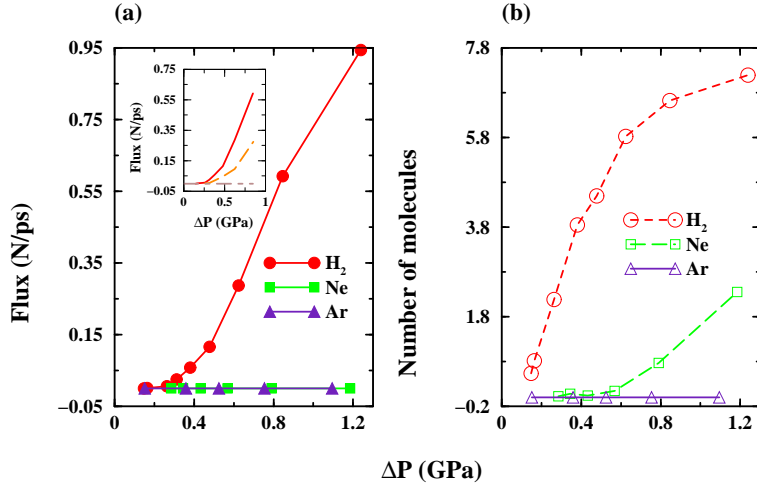


FIG. 3. (Color online) (a): The average flux varied as the function of fluid pressure difference in the single component gases of H_2 , Ne and Ar . Inset: The flux for hydrogen in two different cases. In the first case (long dashed line), the mass of H_2 is artificially enlarged ten times. In the second (dot-dashed line), the interaction of H_2 - H_2 and H_2 -C is replaced by a typical L-J potential. For comparing, the flux for hydrogen in normal condition is also shown (solid line). (b): The average number of molecules located in interspace B.

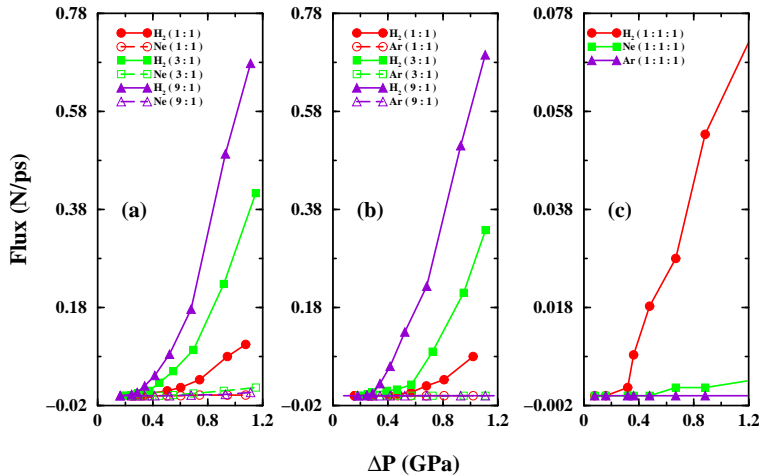


FIG. 4. (Color online) The average flux varied as the function of fluid pressure difference in the multi-component gas molecules. (a) Mixed H_2/Ne with number ratio of 1:1/3:1/9:1. (b) Mixed H_2/Ar with number ratio of 1:1/3:1/9:1. (c) Mixed $H_2/Ne/Ar$ with number ratio of 1:1:1.